



Original Article

The Effect of a Crude Palm Oil–Derived Hybrid Coolant on the Corrosion Behavior of SPCC-Based Electro-Galvanized Steel

Istianto Budhi Rahardja^{1*}, Azhar Basyir Rantawi², Hendra Saputera², Dody⁴, Kartika Tresya Mauriraya⁴, Samsurizal⁵

¹ Sekolah Vokasi, D3, Mechanical Engineering, Institut Teknologi Perusahaan Listrik Negara, Jakarta 11750, Indonesia

² Plantation Processing Technology, Politeknik Kelapa Sawit Citra Widya Edukasi, West Java 17520, Indonesia

⁴ System Information, Institut Teknologi Perusahaan Listrik Negara, Jakarta 11750, Indonesia

⁵ Electrical Engineering, Institut Teknologi Perusahaan Listrik Negara, Jakarta 11750, Indonesia

ARTICLE INFO

Article history:

Received 09 Nov. 2025

Received in revised form

9 Feb. 2026

Accepted : 9 Feb. 2026

Available online 28 Feb. 2026

Keywords:

Bio-based coolant, CPO-derived hybrid coolant, Immersion corrosion test, SPCC-Based Electro-Galvanized Steel, Surface characterization

ABSTRACT

Water-based cooling systems can promote corrosion of metal components, while conventional ethylene glycol coolants pose toxicity and environmental concerns. To address these issues, a novel coolant derived from crude palm oil (CPO) was evaluated for its corrosion behavior on SPCC-based electro-galvanized steel, a material commonly used in radiator applications. The coolant formulation consisted of glycerol, propylene glycol, a CPO-based component, and distilled water, blended to achieve a homogeneous mixture, with chemical analysis confirming three principal natural constituents accounting for nearly the entire formulation. Corrosion performance was assessed by static immersion of SECC samples in the CPO-derived coolant at ambient temperature for 336 h. No measurable weight loss was detected after immersion. SEM–EDS analysis revealed a predominantly zinc-rich surface with no evidence of Fe-rich oxide formation, while XRD patterns were dominated by metallic Zn and Fe reflections at $2\theta \approx 44.6^\circ$, 65.2° , and 82.38° , with no diffraction peaks corresponding to crystalline iron corrosion products such as hematite, magnetite, or goethite. The absence of corrosion-related diffraction features and rust formation indicates that the CPO-based coolant did not induce corrosion under the investigated short-term conditions. These results suggest that the CPO-derived coolant is a promising renewable and corrosion-compatible alternative for cooling applications, although further evaluation under long-term, dynamic, and elevated-temperature conditions is required.

©2026 The Authors. Publishing services by Jurnal Teknik Mesin Mechanical Xplore (JTMMX) on behalf of LPPM UBP Karawang. Open access under the CC BY 4.0 license (<http://creativecommons.org/licenses/by/4.0>).

*Corresponding author.

E-mail address: istianto@itpln.ac.id

Peer review under the responsibility of Editorial Board of Jurnal Teknik Mesin Mechanical Xplore (JTMMX)

1. Introduction

Cooling systems are critical components of industrial machinery, automotive engines, and electronic devices, in which reliable heat dissipation is required to maintain their operational stability and efficiency. In such systems, metallic materials, including radiator panels, cooling channels, and heat exchangers, are continuously exposed to circulating cooling media. Consequently, material degradation due to corrosion is a major engineering concern because it directly affects the thermal efficiency, structural integrity, and service life of cooling system components [1, 2].

<https://doi.org/10.36805/kfp52419>

2746-3672/© 2026 The Authors. Publishing services by Jurnal Teknik Mesin Mechanical Xplore (JTMMX) on behalf of LPPM UBP Karawang. Open access under the CC BY 4.0 license (<http://creativecommons.org/licenses/by/4.0>).

Water-based coolants are widely used because of their low cost, high availability, and favorable thermal properties of water. However, direct contact between water and metallic materials often accelerates corrosion, particularly in steel-based components [3, 4]. Among these, water is widely used because of its low cost, high availability, and favorable thermal properties, such as a high specific heat capacity and thermal conductivity [3-5]. Consequently, water-based cooling systems remain dominant in several industrial and engineering applications.

However, the use of water as a cooling medium is accompanied by inherent limitations related to its compatibility with materials. Direct contact between water and metallic components in cooling systems, such as radiators and cooling channels, can promote corrosion and erosion, particularly under elevated temperatures and continuous flow conditions [6-8]. In practical operations, cooling water circulates through radiators to transfer heat from the system to the environment [8-10]. During prolonged operation, dissolved oxygen, impurities, and temperature gradients in water can accelerate the electrochemical reactions on metal surfaces. These processes may degrade surface integrity, reduce heat transfer performance, and shorten the service life of cooling system components [11, 12].

To overcome these drawbacks, conventional coolants are commonly formulated by adding chemical additives to water to increase the boiling point, provide antifreeze capability, and suppress corrosion. These formulations also aim to stabilize thermal performance under varying operating conditions. Ethylene glycol, which is mainly derived from petroleum resources, is one of the most widely used additives in commercial cooling fluids [13]. Despite their effectiveness, ethylene glycol-based coolants raise concerns regarding toxicity, environmental persistence, and dependence on non-renewable resources. These issues have encouraged research on alternative coolant formulations with improved environmental profiles and performance.

In recent years, increasing attention has been paid to the development of alternative cooling media derived from renewable and environmentally friendly resources. Crude Palm Oil (CPO) and its derivatives, including glycerol and bio-based glycols, have been reported to exhibit favorable lubrication characteristics and potential corrosion-inhibition behavior, making them candidates for coolant formulations [14]. In addition, CPO-derived compounds are biodegradable and can be sourced from renewable feedstocks, thus supporting sustainable engineering. Their polar functional groups may also contribute to the formation of protective films on metal surfaces during cooling-system operation. However, their performance in water-based hybrid coolant systems requires further investigation.

Nevertheless, studies addressing the interactions between CPO-derived hybrid coolants and metallic materials under cooling-relevant conditions remain limited. In particular, SPCC-based electro-galvanized steel, which is widely used in radiator panels and cooling system components, has not been extensively investigated with respect to its corrosion behavior when exposed to CPO-based cooling media. Previous studies on CPO-derived fluids and biodiesel systems have mainly focused on thermal performance, lubrication behavior, and fuel-related properties, whereas systematic evaluations of metal-coolant compatibility are still scarce. Moreover, detailed surface and phase characterizations using scanning electron microscopy coupled with energy-dispersive X-ray spectroscopy (SEM-EDS) and X-ray diffraction (XRD) have rarely been reported for such hybrid coolant systems, especially under static room-temperature conditions representative of early-stage cooling system exposure. Therefore, this study investigates the corrosion behavior of SPCC-based electro-galvanized steel immersed in a hybrid coolant derived from crude palm oil (CPO), in which the coolant composition was first characterized by gas chromatography-mass spectrometry (GC-MS) to ensure compositional stability, followed by mass-loss-based immersion corrosion testing, SEM-EDS analysis to assess surface morphology, elemental distribution, and zinc coating integrity, and XRD analysis to identify potential crystalline corrosion products and phase stability after exposure. By integrating chemical, microstructural, and phase analyses, this work provides a comprehensive assessment of early-stage corrosion behavior and metal-coolant compatibility in CPO-derived hybrid coolants, contributing to the development of sustainable and corrosion-compatible cooling media for industrial and automotive thermal management applications.

2. Methods and Data Collections

2.1. SPCC-based electro-galvanized steel material

Steel plate cold-rolled commercial (SPCC) steel is produced through a cold-rolling process and is widely applied in automotive components (including radiator-related parts), electronic housings, and household appliances owing to its good formability and dimensional accuracy [15-17]. SPCC steel exhibits a smooth surface finish and uniform thickness; however, it is susceptible to corrosion when exposed to aqueous environment. Therefore, SPCC is commonly used as a base material for surface-coated steel in engineering applications to enhance corrosion resistance.

The specimens investigated in this study were supplied under electro-galvanized conditions, corresponding to SECC according to JIS G 3313, with SPCC as the base steel according to JIS G 3141. Therefore, in this study, the material is referred to as SPCC-based electro-galvanized steel.

The physical and mechanical properties of SPCC steel include a density of $7.85 \text{ g}\cdot\text{cm}^{-3}$, tensile strength of approximately 270 Mpa [15, 16], yield strength ranging from 140–280 Mpa [16, 17], elongation at break of 27–31% [17, 18], and thermal conductivity of $73.3 \text{ W}\cdot\text{m}^{-1}\cdot\text{K}^{-1}$. Circular specimens were prepared with a diameter of 35.1 mm and thickness of 1.51 mm. The measured mass of each specimen was approximately 14.33 g, which was consistent with the specimen geometry and the presence of an electro-galvanized zinc coating.

Based on dimensional consistency and surface compositional analysis, the zinc coating thickness was estimated to be on the order of several micrometers to several tens of micrometers, which is consistent with typical electro-galvanized steel (SECC) specifications. Therefore, the contribution of the zinc coating to the overall specimen mass was considered when interpreting the immersion corrosion results.. A typical microstructure of SPCC steel is shown in Figure 1.

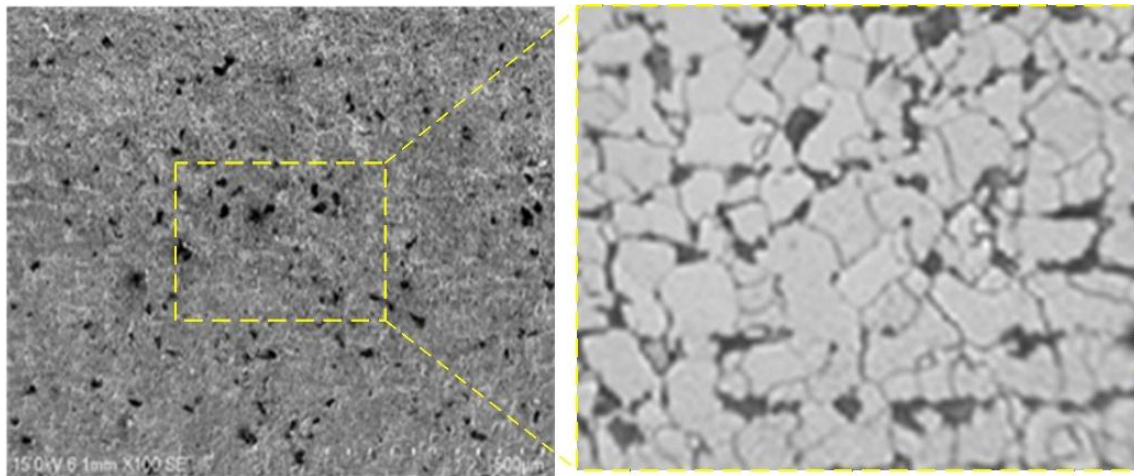


Figure 1. The microstructure of the SPCC-based electro-galvanized cold-rolled surface has a uniform grain structure, smooth finish, and typical ferrite-pearlite phases, which are relevant for evaluating the corrosion behavior in hybrid coolant immersion tests.

2.2. Preparation of CPO-derived hybrid coolant

A hybrid coolant was prepared using CPO derivatives and distilled water. The materials consisted of glycerol (10 mL), propylene glycol (20 mL), a tropical additive (10 mL), and aquadest (70 mL). Aquadest refers to laboratory-grade distilled water, while the tropical component is a CPO-derived additive intended to improve lubrication and corrosion inhibition. All the components were placed in a 150 mL glass beaker, resulting in a total mixture volume of 110 mL.

The initial mixing process was conducted using a magnetic stirrer at room temperature ($27 \pm 2^\circ\text{C}$) for 10 min, as shown in Figure 2. The procedure involved the preparation of the hybrid coolant composition (Figure 2a), placement of the raw materials in a 150 mL glass beaker prior to stirring (Figure 2b), and

subsequent magnetic stirring to achieve a preliminary homogeneous dispersion and uniform distribution of the CPO-derived additives within the aqueous medium (Figure 2c). This initial mixing step was intended to minimize early phase separation and ensure the consistent dispersion of all components before sonication.

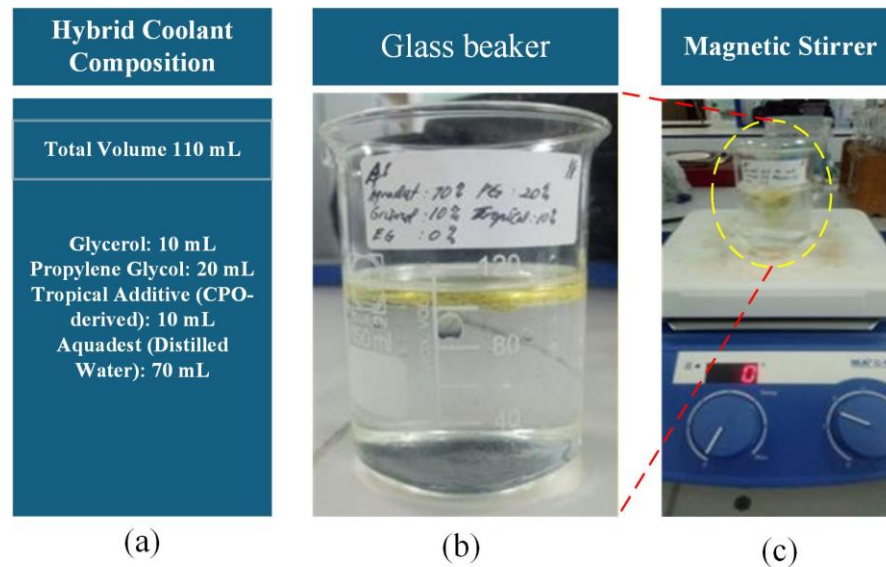


Figure 2. Initial mixing of hybrid coolant components: (a) hybrid coolant compositions, (b) raw materials in a 150 mL glass beaker prior to stirring, and (c) magnetic stirring at room temperature ($27 \pm 2^\circ\text{C}$) for 10 min to achieve preliminary homogeneous dispersion and uniform distribution of CPO-derived additives.

Following the preliminary mixing step, the hybrid coolant was subjected to ultrasonic sonication to further promote uniform dispersion of the CPO-derived components within the aqueous phase. Sonication was performed in the pulse mode at 60°C for 60 min using an ultrasonic bath, as shown in Figure 3a. The objective of this sonication step was to improve the visual homogeneity of the hybrid coolant by enhancing the molecular-level dispersion and reducing the macroscopic phase separation between the hydrophilic constituents (aqueous solution and glycerol) and organic CPO-derived additives (Figure 3b).

After sonication, the glass beaker containing the hybrid coolant was removed from the ultrasonic unit and allowed to cool to ambient temperature. The final appearance of the hybrid coolant after sonication is shown in Figure 3c, where a visually homogeneous and stable mixture was obtained after sonication. The absence of visible phase separation after cooling indicates that the preparation procedure achieved its intended objective and produced a hybrid coolant suitable for subsequent immersion corrosion testing and chemical characterization

2.3. Gas chromatography–mass spectrometry (GC–MS)

Gas chromatography–mass spectrometry (GC–MS) analysis was performed to characterize the chemical constituents of the CPO-derived hybrid coolant prior to immersion corrosion testing. Before analysis, the aqueous phase was separated from the organic components using liquid–liquid extraction with n-hexane to reduce water interference and enhance the detection of organic compounds.

GC–MS measurements were performed using an Agilent GC–MS system (GCMSD 5973) equipped with an HP-5MS capillary column ($30\text{ m} \times 0.25\text{ mm} \times 0.25\text{ }\mu\text{m}$). Helium was used as the carrier gas at a constant flow rate of $1.0\text{ mL}\cdot\text{min}^{-1}$. The injection volume was $1\text{ }\mu\text{L}$, and the system was operated in split mode with a split ratio of 10:1. The oven temperature program was set from 50°C (held for 2 min) to 280°C at a heating rate of $10^\circ\text{C}\cdot\text{min}^{-1}$.

2.4. Immersion corrosion test conditions

Immersion corrosion tests were conducted to evaluate the corrosion behavior of the SPCC-based electrogalvanized CPO-derived hybrid coolant using a mass loss-based approach. Prior to immersion, all

specimens were mechanically cleaned, rinsed with distilled water, dried, and weighed using an analytical balance with a resolution of 0.01 mg to obtain the initial mass (m_0). The average initial mass of the specimens was 14.33 g. The exposed surface area (A) of each specimen was determined based on the dimensions of the specimen measured before testing.

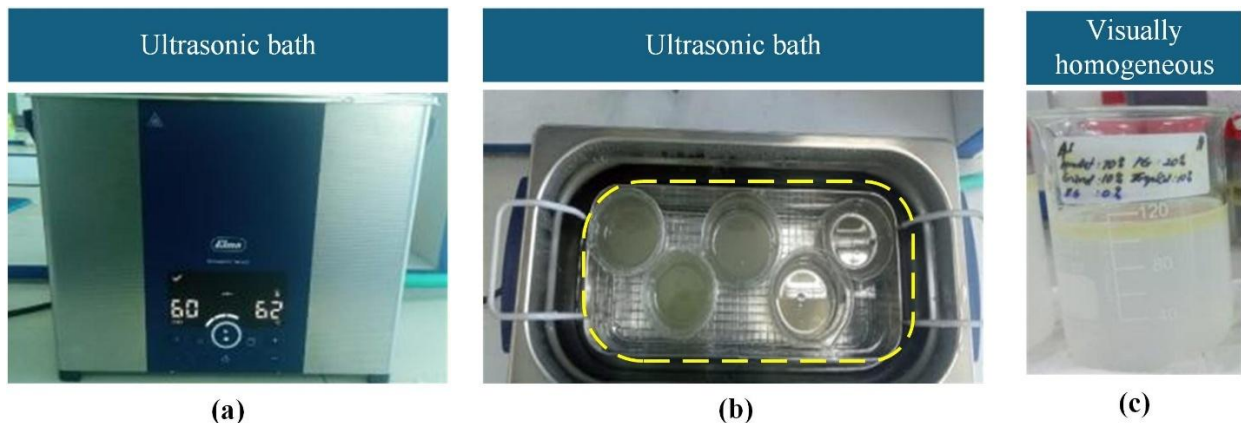


Figure 3. Ultrasonic homogenization and final appearance of hybrid coolant: (a) ultrasonic bath with the glass beaker containing the hybrid coolant prior to sonication, (b) sonication performed in pulse mode at 60°C for 60 min to enhance molecular-level dispersion and improve the colloidal stability of CPO-derived additives, (c) final hybrid coolant after sonication.

The specimens were immersed under static conditions at room temperature ($27 \pm 2^\circ\text{C}$) for 336 h (14 d), which is commonly adopted for preliminary corrosion evaluation in coolant-related studies. Three specimens ($n = 3$) were used for each test condition to ensure repeatability. In addition to the hybrid coolant, control samples were prepared by immersing SPCC steel in distilled water and a commercial ethylene glycol-based coolant. The weighing procedure and immersion test setup are illustrated in Figure 4.

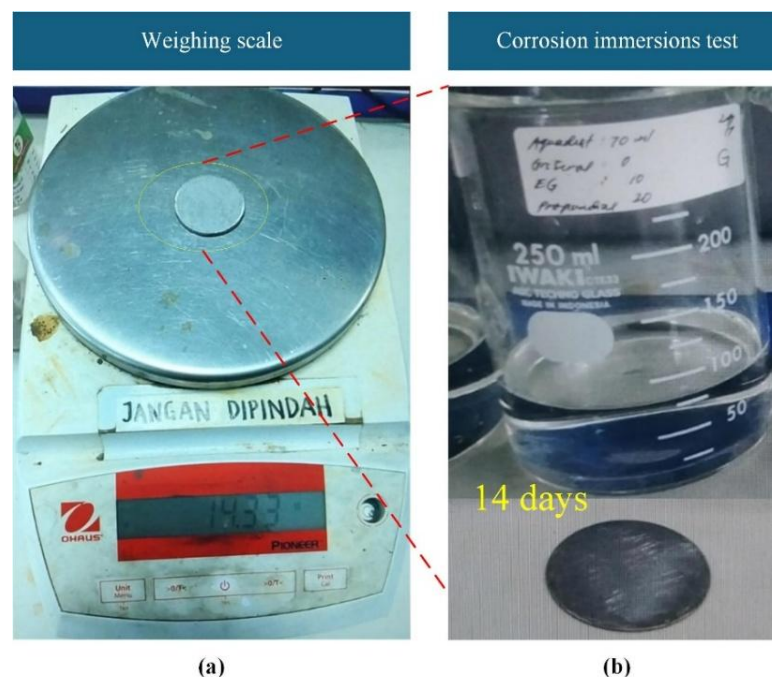


Figure 4. Immersion corrosion test procedure of SPCC steel: (a) weighing of SPCC specimens using an analytical balance prior to immersion to obtain the initial mass (m_0), and (b) static immersion corrosion test of SPCC specimens in the CPO-derived hybrid coolant and control media at room temperature ($27 \pm 2^\circ\text{C}$) for 336 h.

During immersion, the specimens were fully submerged without mechanical agitation, and aeration was limited to ambient conditions. After the immersion period, the specimens were removed, rinsed with distilled water to eliminate residual coolant, dried at 40°C for 30 min, and allowed to equilibrate in a

desiccator. The final mass (m_t) of each specimen was measured using an analytical balance. The mass loss (Δm) was calculated using Eq. (1):

$$\Delta m = m_0 - m_t \quad (1)$$

where m_0 is the initial mass before immersion and m_t is the final mass after immersion.

The corrosion rate (CR) was estimated using the mass-loss-based expression given in Eq. (2):

$$CR = \frac{K \cdot \Delta m}{A \cdot t \cdot \rho} \quad (2)$$

where CR is the corrosion rate ($\text{mm} \cdot \text{year}^{-1}$), Δm is the mass loss (g), A is the exposed surface area of the specimen (cm^2), t is the immersion time (h), ρ is the density of SPCC steel ($7.85 \text{ g} \cdot \text{cm}^{-3}$), and K is a dimensional constant (8.76×10^4) used to convert units to $\text{mm} \cdot \text{year}^{-1}$.

2.5. Electron microscopy (SEM–EDS)

The surface morphology and elemental composition of the SPCC-based electrogalvanized steel specimens after immersion were examined using SEM imaging. SEM observations at 280°C were conducted at an accelerating voltage of 15 kV. Prior to analysis, the specimens were coated with a thin conductive layer to minimize charging effects. Elemental analysis was performed using an EDS detector integrated with the SEM. EDS measurements were conducted at an accelerating voltage of 15–20 kV and a working distance of 10 mm. The elemental composition was analyzed in selected regions of interest to assess the surface degradation and corrosion-related features.

2.6. X-ray Diffraction

The XRD analysis was conducted to identify possible crystalline corrosion products and phase changes on the surface of SPCC-based electro-galvanized steel after immersion in the CPO-derived hybrid coolant. XRD measurements were performed at room temperature using a diffractometer equipped with Cu $K\alpha$ radiation ($\lambda = 1.5406 \text{ \AA}$). Diffraction patterns were collected over a 2θ range of 20–80°, with a step size of 0.02° and a scanning speed of 2°·min⁻¹. Phase identification was carried out by comparing the obtained diffraction patterns with standard reference databases.

XRD analysis was employed to complement the SEM–EDS observations by providing phase-level information on the surface condition after immersion, particularly to determine whether exposure to the hybrid coolant induced the formation of crystalline corrosion products or altered the original metallic phases. Through the combined use of SEM–EDS and XRD, both surface morphology, elemental distribution, and phase stability of the electro-galvanized steel were systematically evaluated following coolant exposure.

3. Results and Discussion

3.1. Chemical characterization of CPO-derived hybrid coolant analysis

Gas chromatography–mass spectrometry (GC–MS) was used to characterize the chemical composition of the CPO-derived hybrid coolant prior to corrosion testing. Chemical characterization is essential to ensure formulation consistency and support the interpretation of subsequent metal–coolant interactions.

The GC–MS chromatogram revealed eight detectable peaks, of which three dominant peaks accounted for approximately 99.25% of the total area. The primary peak was observed at a retention time of 8.614 min, which represented 59.07% of the total area. The second and third major peaks appeared at retention times of 2.566 min and 2.761 min, contributing 27.93% and 12.25%, respectively. All remaining peaks accounted for less than 0.5% of the total area, indicating that they were present only at trace levels. The GC–MS peak area distributions are summarized in [Table 1](#).

The predominance of three major peaks demonstrates that the hybrid coolant possesses a chemically

simple, well-defined, and stable composition with minimal formation of secondary or degradation-related compounds. Such compositional simplicity is advantageous for corrosion studies because it reduces the uncertainty associated with reactive minor species that may influence the electrochemical behavior.

Table 1. GC–MS peak area distribution of the CPO-derived hybrid coolant

Parameters	Peak No.							
	1	2	3	4	5	6	7	8
Retention time (min)	2.57	2.76	8.61	16.84	18.57	19.28	20.77	23.86
Area fraction (%)	27.93	12.25	59.07	0.33	0.23	0.07	0.05	0.08

Detailed GC–MS peak area distributions have rarely been reported in corrosion-focused studies involving bio-based or hybrid fluids. For instance, Jin et al. [19] and Kugelmeier et al. [20] primarily characterized biodiesel and biofuel systems using bulk parameters, such as ester content, total acid number, viscosity, and water content, without presenting retention time–resolved chromatographic data. In contrast, Wang and Liu [21] reported chemically complex bio-oil systems characterized by diverse oxygenated and acidic compounds, which were associated with severe corrosion rates exceeding $0.1\text{--}1\text{ mm}\cdot\text{year}^{-1}$. Compared to these systems, the CPO-derived hybrid coolant examined in this study exhibited a markedly lower compositional complexity, as evidenced by the dominance of a limited number of stable organic constituents.

From a physicochemical perspective, the dominance of stable, nonionic organic components and the low proportion of reactive minor species suggest limited electrochemical activity at the metal–coolant interface of the CWS. CPO-derived organic molecules may adsorb onto steel surfaces through weak physical interactions, forming a discontinuous protective layer that reduces direct metal–aqueous contact and suppresses early stage uniform corrosion. Similar behavior has been reported for chemically stable cooling fluids under static exposure conditions [22].

Overall, the GC–MS results confirmed that the CPO-derived hybrid coolant exhibited high chemical stability and low compositional complexity. This provides a reliable foundation for correlating fluid chemistry with the corrosion behavior of SPCC-based electro-galvanized steel, which is systematically evaluated in the following sections.

3.2. Immersion corrosion analysis

The mass-loss-based corrosion test in this study showed that SPCC-based electro-galvanized steel did not lose any measurable mass after 336 h (14 d) of static immersion in the CPO-based hybrid coolant at room temperature. The measured mass difference (Δm) was too small for detection. Consequently, the corrosion rate (CR) was almost zero. This indicates that there was almost no corrosion during the short-term static exposure period.

This behavior is consistent with previous studies reporting that the corrosion of carbon steel in bio-based or organic fluids is strongly governed by the chemical aggressiveness of the medium. Under mild chemical conditions, Kugelmeier et al. [20] reported no measurable mass loss for carbon steel immersed in biodiesel–petrodiesel blends (B7–B30) after 2160 h at $50\text{ }^{\circ}\text{C}$, with only minor surface morphology changes and no continuous corrosion layers. In contrast, studies conducted in chemically aggressive bio-oil environments have consistently reported substantially higher corrosion rates.

In contrast, studies conducted in chemically aggressive bio-oil environments have reported significantly higher corrosion rates. Wang and Liu [21] observed corrosion rates exceeding $1\text{ mm}\cdot\text{year}^{-1}$ for carbon steel exposed to raw bio-oil and bio-oil-methanol mixtures at $50\text{ }^{\circ}\text{C}$. SEM analysis revealed thick corrosion layers, and XRD identified the iron-oxide phases. Similarly, Andari et al. (2022) [23] reported very high corrosion rates exceeding $10\text{ mm}\cdot\text{year}^{-1}$ for carbon and low-alloy steels exposed to acidic vegetable oils and fatty acid-rich media. These results confirm that acidity and fatty acids significantly accelerate the corrosion rate.

Additional evidence is provided by biodiesel corrosion studies. Hu et al. [24] reported measurable corrosion of magnesium, aluminum, and carbon steel in rapeseed-oil-based biodiesel. SEM observations revealed localized corrosion and surface roughening in the samples after the tests. The severity of corrosion is governed by the acidity and impurity content of the oil. Jin et al. [19] also observed corrosion products and surface deposits on carbon steel exposed to palm biodiesel. This occurred even when the bulk fuel properties were within an acceptable range. These studies indicate that corrosion in bio-based fluids is often controlled by trace impurities rather than the dominant organic components.

Compared with these aggressive environments, the CPO-derived hybrid coolant investigated in this study represents a considerably milder environment. The coolant comprised a neutral aqueous phase with a controlled organic composition. The tests were conducted at ambient temperature under static conditions. These factors suppress corrosion-driven electrochemical reactions. The absence of measurable mass loss and near-zero corrosion rate observed in this study are consistent with these conditions.

3.3. SEM-EDS surface morphology

SEM-EDS analysis was conducted to examine the surface morphology and elemental composition of SPCC-based electro-galvanized steel after 336 h of static immersion in the CPO-derived hybrid coolant. Figure 5a–c show the SEM micrographs and corresponding EDS point analyses obtained from three representative surface regions selected to evaluate the local variations in the surface condition following immersion. The EDS results are reported in terms of weight concentration (wt.%), as provided by the instrument software.

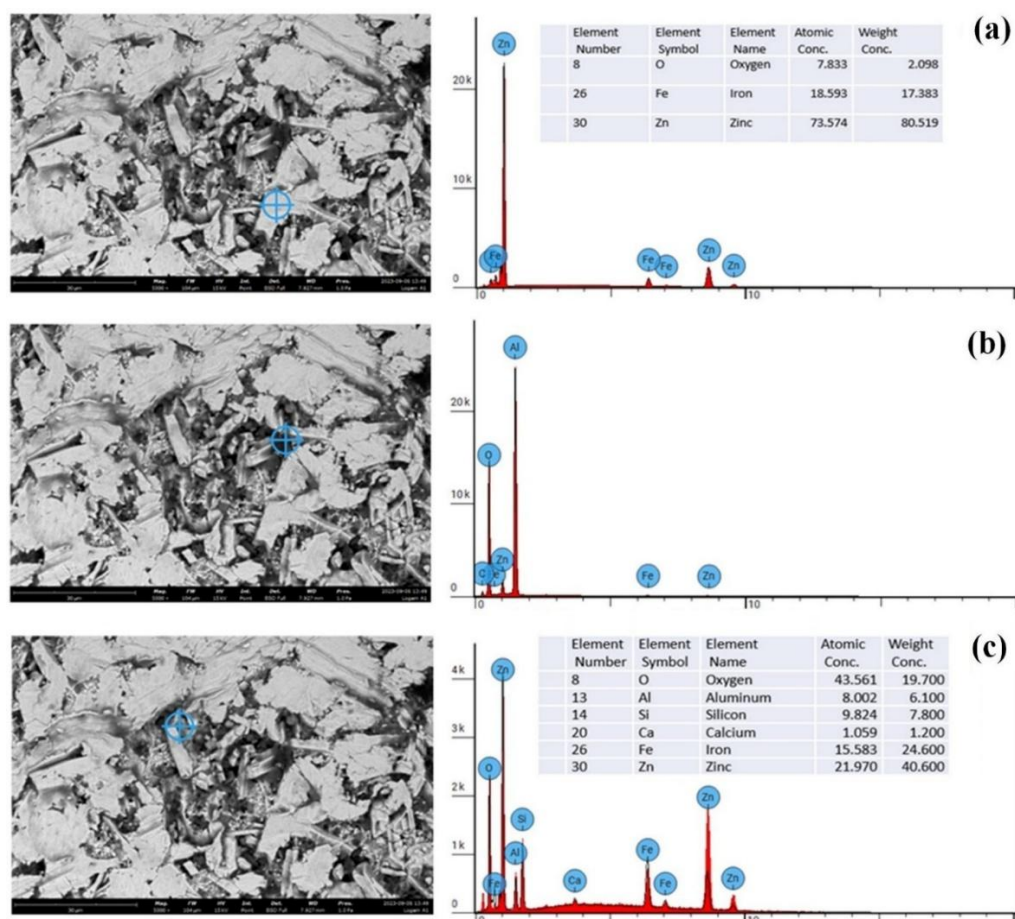


Figure 5. SEM-EDS microscopy analyses of SPCC-based electro-galvanized steel (SECC) after 336 h of static immersion in CPO-derived hybrid coolant: (a) Zn-rich surface region, (b) stable zinc-coated surface with minor elemental variations, and (c) heterogeneous surface region containing Zn, Fe, O, and trace elements.

As shown in Figure 5a, the surface was dominated by zinc, with Zn accounting for approximately 80.5

wt. %, while Fe is detected at a comparatively lower level (17.4 wt.%). The oxygen content was relatively low (2.1 wt.%), indicating the absence of thick iron oxide layers. These results confirm that the zinc coating remained intact in this region and effectively shielded the underlying steel substrate from direct exposure to coolant. The surface morphology observed in [Figure 5b](#) is characterized by irregular block-like features similar to those shown in [Figure 5a](#). The EDS spectra indicated that Zn was the primary metallic element, accompanied by oxygen and minor Al. No localized enrichment of Fe–O species was observed, suggesting that active corrosion of the steel substrate did not occur and that the zinc-coated layer remained intact. As shown in [Figure 5c](#), a heterogeneous distribution of elements was observed. Although Zn remains a significant component (≈ 40.6 wt. %), a higher oxygen content (≈ 19.7 wt.%) and minor elements such as Al, Si, and Ca are detected. These elements are attributed to superficial surface deposits or environmental residues rather than corrosion products. Importantly, Fe was present at a moderate level (≈ 24.6 wt. %) without evidence of Fe-rich oxide formation, indicating that the steel substrate was not significantly corroded. Therefore, this region is interpreted as a transition zone between the Zn coating and surface deposits.

To facilitate a comparative interpretation of the SEM–EDS results across the analyzed regions, the main observations from [Figure 5a–c](#) are summarized in [Table 2](#).

Table 2. Summary of SEM–EDS interpretation of SPCC-based electro-galvanized steel after immersion in NaCl solution.

Aspect	Spot 1	Spot 2	Spot 3
Zn dominance	Very high	High	Moderate
Fe contribution	Low	Low–moderate	Moderate
Thick iron oxide layer	Not observed	Not observed	Not observed
Evidence of pitting	None	None	None
Coating condition	Intact	Intact	Transition zone

Overall, the SEM–EDS results demonstrate that Zn remained the dominant surface element across all the analyzed regions, confirming the persistence of the electro-galvanized layer after 336 h of static immersion. The absence of Fe-rich oxide layers, pitting corrosion, and severe surface degradation is consistent with the negligible mass loss observed during immersion testing. These findings indicate that the CPO-derived hybrid coolant did not induce significant corrosion of the SPCC-based electrogalvanized steel under the investigated conditions. The SEM–EDS observations obtained in this study further provide a basis for comparison with previously published studies on carbon steel and zinc-coated steel exposed to bio-based fluids, cooling media, and organic environments, as discussed in the next section.

3.4. XRD analysis

X-ray diffraction (XRD) analysis was conducted to identify crystalline corrosion products formed on the surface of SPCC-based electro-galvanized steel after 336 h of static immersion in the CPO-derived hybrid coolant. The diffraction patterns were dominated by reflections corresponding to metallic Zn and Fe phases, indicating that the galvanized steel structure remained largely intact after immersion.

No diffraction peaks associated with crystalline iron corrosion products—such as Fe_2O_3 , Fe_3O_4 , or $\text{FeO}(\text{OH})$ —were detected within the resolution limits of the XRD measurements. The main diffraction peaks of the immersed samples appeared at 2θ values of approximately 44.6° , 65.2° , and 82.38° , which are characteristic of metallic phases. In contrast, hematite (JCPDS No. 33-0664) exhibits characteristic peaks at 24.12° , 33.15° , 40.48° , and 54.08° , none of which were observed in the present study ([Figure 6](#)).

Under more aggressive exposure conditions, Jin et al. [19] reported the formation of various crystalline corrosion products on mild steel immersed in palm biodiesel, including Fe_2O_3 , $\text{FeO}(\text{OH})$, FeCO_3 , FeO , and $\text{Fe}_2\text{O}_2\text{CO}_3$. In contrast, Wang and Liu [21] observed only base-metal diffraction peaks in bio-oil environments, attributing the absence of corrosion products to the formation of ultrathin or amorphous

surface layers beyond the detection capability of XRD.

The present results are consistent with the latter findings, suggesting that the CPO-derived hybrid coolant environment was relatively mild. The absence of detectable crystalline corrosion phases indicates that corrosion progression was limited and did not result in the formation of bulk or crystalline corrosion products. Nevertheless, the presence of amorphous or nanoscale corrosion layers cannot be completely excluded due to the inherent limitations of XRD.

Overall, the XRD results are in good agreement with the negligible mass loss and SEM–EDS observations, confirming that no significant corrosion-related phase transformations occurred under the investigated static immersion conditions..

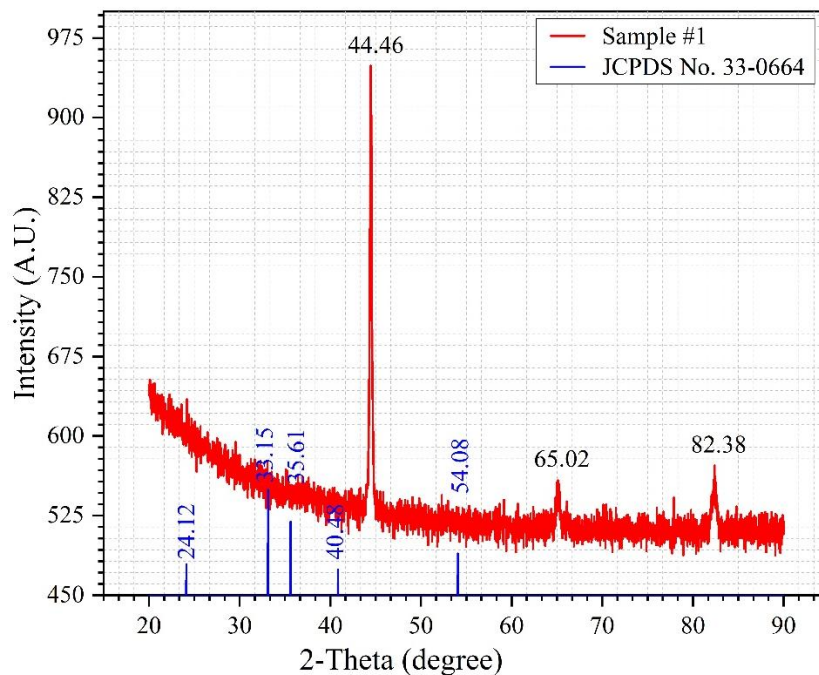


Figure 6. XRD patterns of SPCC-based electro-galvanized steel after 336 h of static immersion in the CPO-derived hybrid coolant, showing dominant metallic Zn and Fe phases and the absence of detectable crystalline iron corrosion products

3.5. Comparison with previous studies

The corrosion behavior observed in the present study is consistent with that reported for carbon steel exposed to relatively mild bio-based or organic fluid environments. As summarized in Table 3, several studies have shown that under non-aggressive conditions, mass loss may remain below gravimetric detection limits, even after prolonged exposure. Kugelmeier et al. [20] reported no measurable mass loss for carbon steel immersed in biodiesel–petrodiesel blends (B7–B30) after 2160 h at 50 °C, with SEM observations indicating only minor surface changes and no formation of thick corrosion layers. A similar trend was observed in the present study, where the SPCC-based electro-galvanized steel exhibited no measurable mass loss after 336 h of static immersion, and SEM–EDS analysis confirmed the persistence of a Zn-dominated surface without the formation of Fe-rich oxide.

In contrast, studies conducted under chemically aggressive bio-based environments consistently report significant corrosion rates and pronounced surface degradation. Wang and Liu [21] documented corrosion rates exceeding $1 \text{ mm}\cdot\text{year}^{-1}$ for carbon steel exposed to raw bio-oil and bio-oil–methanol mixtures at 50°C, where SEM revealed uniform corrosion and thick corrosion layers, and XRD identified iron-oxide phases. More severe corrosion was reported by Andari et al. [23], who observed corrosion rates above $10 \text{ mm}\cdot\text{year}^{-1}$ for carbon and low-alloy steels immersed in acidic vegetable oils and fatty acid-rich media.

Table 3. Comparison of the corrosion behavior of metallic materials exposed to various aggressive and bio-based environments, including chloride solutions, biodiesel, bio-oil systems, circulating cooling water, and the CPO-derived hybrid coolant investigated in the present study. The table summarizes the test conditions, exposure durations, surface and phase characterization results, and reported corrosion rates.

No.	Author(s) & Year	Tested Material(s)	Corrosion Test Medium	Test Duration / Exposure Time	SEM / SEM-EDS Findings	XRD Findings	Corrosion Rate / Main Corrosion Outcome
1	Solehudin et al. (2025) [1]	Carbon steel with Zn and ZnAl coatings	A NaCl solution (1–5 wt.%)	Up to 720 h (30 days)	ZnAl showed smoother surface, fewer pits (<300 nm), stable morphology; Zn showed white rust and deeper pits	Not reported	Zn: $\sim 7.89 \mu\text{m}\cdot\text{y}^{-1}$; ZnAl: $\sim 1.03 \mu\text{m}\cdot\text{y}^{-1}$
2	Wang & Liu, 2024 [21]	Carbon steel	Raw bio-oil and bio-oil-methanol mixtures	168 h (7 days) at 50°C	Severe uniform corrosion; thick corrosion layers observed	Iron-oxide phases detected	$>1 \text{ mm}\cdot\text{year}^{-1}$ at 50 °C
3	Balci, 2024 [25]	Ni20Ti50Sn30 alloy	Simulated body fluid (SBF)	14 days	SEM-EDS confirmed formation of protective TiO ₂ layer	B2, B19', Ti ₂ Ni, TiNiSn phases identified	$2.16 \times 10^{-4} \text{ mm}\cdot\text{year}^{-1}$ (very high corrosion resistance)
4	Kugelmeier et al., 2022 [20]	Carbon steel	Biodiesel-petrodiesel blends (B7–B30)	2160 h (90 days) at 50°C	Minor surface changes; no severe corrosion layers	Not reported	No measurable mass loss after 2160 h at 50 °C
5	Yang et al., 2021 [22]	Carbon steel (20# steel)	Circulating cooling water (with aeration and microbial activity)	90 days	Not reported	Not reported	$0.01552\text{--}0.03589 \text{ mm}\cdot\text{year}^{-1}$
6	Andari et al. 2022 [23]	AISI 1018 carbon steel, A387 Gr11 low-alloy steel, AISI 316L stainless steel	Vegetable oils, waste oils, PFAD, TOFA, DTO, and oleic-acid model mixtures	168–720 h at elevated temperature	Uniform corrosion and severe metal dissolution observed in high-FFA oils	Not reported	Carbon and low-alloy steels: very high corrosion rates ($>10 \text{ mm}\cdot\text{year}^{-1}$); AISI 316L: negligible corrosion
7	Jin et al., 2015 [19]	Carbon steel	Palm biodiesel	NR	SEM showed corrosion products and surface deposits	Not reported	Detectable corrosion due to FFA and water content
8	Hu et al., 2011 [24]	Magnesium, aluminum, carbon steel	Biodiesel (rapeseed oil-methanol)	NR	SEM revealed localized corrosion and surface roughening	Not reported	Measurable corrosion influenced by acidity and impurities
9	Present study	SPCC-based electro-galvanized steel (SECC, Zn-coated)	CPO-derived hybrid coolant (water-propylene glycol-glycerol-CPO additive)	336 h (14 days) at room temperature, static condition	SEM-EDS showed intact surface morphology dominated by Zn; no Fe-rich oxide layers, pitting corrosion, or coating delamination detected	No corrosion-induced crystalline phases detected; no Fe-oxide phases observed	No measurable mass loss; corrosion rate $\approx 0 \text{ mm}\cdot\text{year}^{-1}$ (within gravimetric detection limit)

Intermediate corrosion behavior has been reported in biodiesel systems containing varying levels of impurities. Hu et al. [24] observed measurable corrosion and localized surface roughening on magnesium, aluminum, and carbon steel exposed to rapeseed-oil-based biodiesel, while Jin et al. [19] reported the formation of corrosion products and surface deposits on carbon steel immersed in palm biodiesel. In both cases, corrosion was primarily attributed to the presence of free fatty acids, water, and oxidation byproducts rather than the bulk fuel itself. These findings indicate that corrosion in bio-based fluids is often governed by minor reactive species and environmental aggressiveness rather than the base fluid composition alone.

Compared to these biodiesel and bio-oil systems, the CPO-derived hybrid coolant investigated in this study represents a significantly milder environment. The neutral aqueous phase, controlled organic composition, and absence of highly acidic components suppressed the corrosion-driving electrochemical reactions. The preservation of the zinc coating and the absence of measurable mass loss indicate superior material compatibility between the hybrid coolant and SPCC-based electro-galvanized steel under static conditions. This comparison confirmed that the formulated coolant provided a chemically stable environment during short-term exposure, whereas long-term and dynamic condition evaluations are required for a comprehensive durability assessment.

4. Conclusion

This study evaluated the corrosion behavior of SPCC-based electro-galvanized steel immersed in a crude palm oil (CPO)-derived hybrid coolant under static room-temperature conditions using mass-loss measurements, SEM–EDS surface analysis, and X-ray diffraction (XRD). No measurable mass loss was detected after 336 h of immersion, corresponding to a corrosion rate of approximately $0 \text{ mm}\cdot\text{year}^{-1}$ within the gravimetric detection limit. SEM–EDS results showed that the steel surface remained predominantly zinc-rich (up to $\sim 80.5 \text{ wt.}\%$) with low oxygen content ($\sim 2 \text{ wt.}\%$), and no evidence of Fe-rich oxide formation, pitting corrosion, or coating delamination, while XRD patterns were dominated by metallic Zn and Fe reflections at $2\theta \approx 44.6^\circ$, 65.2° , and 82.38° , with no detectable crystalline iron corrosion products such as hematite, magnetite, or goethite. The favorable corrosion performance is attributed to the chemically stable coolant composition, as confirmed by GC–MS analysis in which three major constituents accounted for $\sim 99.25\%$ of the total chromatographic area, together with the mild exposure conditions, including a neutral aqueous phase, controlled organic composition, ambient temperature, and limited oxygen availability. Overall, the combined findings demonstrate that the CPO-derived hybrid coolant exhibits good short-term corrosion compatibility with SPCC-based electro-galvanized steel under static conditions, although further validation under long-term exposure, dynamic flow, and elevated-temperature conditions is required for practical automotive and industrial applications.

Author's Declaration

Authors' contributions

Istianto Budhi Rahardja: Conceptualization, Methodology, Formal analysis, Data curation, Writing – original draft, Writing – review & editing. Azhar Basyir Rantawi: Methodology, Investigation, Validation, Writing – review & editing. Hendra Saputera: Investigation, Data curation, Visualization. Dody: Investigation, Resources, Validation. Kartika Tresya Mauriraya: Data curation, Visualization, Writing – review & editing. Samsurizal: Supervision, Project administration, Writing – review & editing.

Acknowledgment

The authors declare that this research did not receive any specific grant from funding agencies in the public, commercial, or not-for-profit sectors.

Availability of data and materials

All data supporting the findings of this study are available from the corresponding author upon reasonable request.

Competing interests

The authors declare no conflicts of interest related to this study.

References

- [1] M. I. Maulana, R. Ragadhita, H. Salam, and A. Solehudin, "Investigating the corrosion behavior of hot-dip galvanized Zn and Zn-10Al coatings on carbon steel without top coating in chloride-rich immersion environments," *Mechanical Engineering for Society and Industry*, vol. 5, no. 2, pp. 367-384, 2025. doi: <https://doi.org/10.31603/mesi.13743>
- [2] V. Madeshwaren, N. Selvapalam, S. Mahadevan, and D. K. Vairavel, "Evaluation of corrosion mitigation of SS904l using inhibitors with statistical and morphological analysis," *Mechanical Engineering for Society and Industry*, vol. 5, no. 1, pp. 91-106, 2025. doi: <https://doi.org/10.31603/mesi.12519>
- [3] B. Liščić, H. M. Tensi, and W. Luty, *Theory and Technology of Quenching (A Handbook)*. Berlin, Heidelberg: Springer, 2014.
- [4] W. Luty, "Types of Cooling Media and Their Properties," in *Theory and Technology of Quenching: A Handbook*, B. Liščić, H. M. Tensi, and W. Luty, Eds. Berlin, Heidelberg: Springer Berlin Heidelberg, 1992, pp. 248-340.
- [5] S. He, H. Gurgenci, Z. Guan, X. Huang, and M. Lucas, "A review of wetted media with potential application in the pre-cooling of natural draft dry cooling towers," *Renewable and Sustainable Energy Reviews*, vol. 44, pp. 407-422, 2015/04/01/ 2015. doi: <https://doi.org/10.1016/j.rser.2014.12.037>
- [6] J. Steven Brown and P. A. Domanski, "Review of alternative cooling technologies," *Applied Thermal Engineering*, vol. 64, no. 1, pp. 252-262, 2014/03/01/ 2014. doi: <https://doi.org/10.1016/j.applthermaleng.2013.12.014>
- [7] S. K. Das, "Nanofluids—The Cooling Medium of the Future," *Heat Transfer Engineering*, vol. 27, no. 10, pp. 1-2, 2006/12/01 2006. doi: 10.1080/01457630600904585
- [8] M. Ismail, M. Yebiyoy, and I. Chaer, "A Review of Recent Advances in Emerging Alternative Heating and Cooling Technologies," *Energies*, vol. 14, no. 2, p. 502. doi: <https://doi.org/10.3390/en14020502>
- [9] R. W. Lutey, "Process cooling water," in *Handbook of Biocide and Preservative Use*, H. W. Rossmoore, Ed. Dordrecht: Springer Netherlands, 1995, pp. 50-82.
- [10] D. A. Meier, B. Chen, and C. Myers, "Chapter 11 - Cooling water systems: An overview," in *Water-Formed Deposits*, Z. Amjad and K. D. Demadis, Eds.: Elsevier, 2022, pp. 239-267.
- [11] E. Klimesmith Dawn, H. McCuen Richard, and P. Albrecht, "Effect of Environmental Conditions on Corrosion Rates," *Journal of Materials in Civil Engineering*, vol. 19, no. 2, pp. 121-129, 2007/02/01 2007. doi: [https://doi.org/10.1061/\(ASCE\)0899-1561\(2007\)19:2\(121\)](https://doi.org/10.1061/(ASCE)0899-1561(2007)19:2(121))
- [12] R. E. Melchers, "The effect of corrosion on the structural reliability of steel offshore structures," *Corrosion Science*, vol. 47, no. 10, pp. 2391-2410, 2005/10/01/ 2005. doi: <https://doi.org/10.1016/j.corsci.2005.04.004>
- [13] W. N. Mutuku, "Ethylene glycol (EG)-based nanofluids as a coolant for automotive radiator," *Asia Pacific Journal on Computational Engineering*, vol. 3, no. 1, p. 1, 2016/06/21 2016. doi: <https://doi.org/10.1186/s40540-016-0017-3>
- [14] G. E. Totten, H. M. Tensi, and K. Lainer, "Performance of vegetable oils as a cooling medium in comparison to a standard mineral oil," *Journal of Materials Engineering and Performance*, vol. 8,

- no. 4, pp. 409-416, 1999/08/01 1999. doi: <https://doi.org/10.1361/105994999770346693>
- [15] D. Mulyadi, A. Amir, A. Cepi Budiansyah, S. Sukarman, K. Khoirudin, L. Arif Wibowo, and S. Kumbarasari, "The Box-Behnken Response Surface Methodology Approach to Optimize Tensile Strength Load in Resistance Spot Welding Using SPCC-SD Steel," *Jurnal Teknik Mesin Mechanical Xplore*, vol. 4, no. 2, pp. 47-60, 2024. doi: <https://doi.org/10.36805/jtmmx.v4i2.6090>
- [16] K.-J. Fann and Y.-H. Wu, "On Forming Sheet Metal Parts in Single Curvature with English Wheel," in *Proceedings of the 14th International Conference on the Technology of Plasticity - Current Trends in the Technology of Plasticity*, Cham, 2024, pp. 274-284: Springer Nature Switzerland. doi: https://doi.org/10.1007/978-3-031-40920-2_29
- [17] Sukarman, M. Taufik Ulhakim, K. Khoirudin, D. Mulyadi, A. Amir, A. Suhara, and N. Rahdiana, "A Comprehensive Study on Production Efficiency Enhancement Using Optimal Power Press Tonnage in Stamping," *Jurnal Teknik Mesin Mechanical Xplore*, vol. 5, no. 2, pp. 69-78, 2025. doi: <https://doi.org/10.36805/jtmmx.v5i2.8048>
- [18] T. C. Pratama, S. Sukarman, G. Tikamori, D. Mulyadi, A. Supriyanto, A. Amir, K. Khoirudin, and A. Hananto, "The Advanced Analysis of Deep Drawing Processes for 1-Inch Diameter Dop-Pipe Caps: Simulation and Experimental Insights," (in en_US), *Jurnal Teknik Mesin Mechanical Xplore*, vol. 5, no. 1, pp. 1-12, 2024. doi: <https://doi.org/10.36805/jtmmx.v5i1.7269>
- [19] D. Jin, X. Zhou, P. Wu, L. Jiang, and H. Ge, "Corrosion behavior of ASTM 1045 mild steel in palm biodiesel," *Renewable Energy*, vol. 81, pp. 457-463, 2015. doi: <https://doi.org/10.1016/j.renene.2015.03.022>
- [20] C. L. Kugelmeier, M. R. Monteiro, R. da Silva, S. E. Kuri, V. L. Sordi, and C. A. Della Rovere, "Corrosion behavior of carbon steel, stainless steel, aluminum and copper upon exposure to biodiesel blended with petrodiesel," *Energy*, vol. 226, 2021. doi: <https://doi.org/10.1016/j.energy.2021.120344>
- [21] H. Wang and J. Liu, "Electrochemical corrosion study of carbon steel in bio-oil environments," *Renewable Energy*, vol. 221, 2024. doi: <https://doi.org/10.1016/j.renene.2023.119823>
- [22] Y. Yang, J. Li, Q. Gu, and X. Yuan, "Study on microbial corrosion inhibition of carbon steel in circulating cooling water system," *IOP Conference Series: Earth and Environmental Science*, vol. 692, no. 3, 2021. doi: <https://doi.org/10.1088/1755-1315/692/3/032108>
- [23] F. Andari, J. Kittel, J. Fernandes, N. Godin, B. Ter-Ovanesian, and F. Ropital, "High temperature corrosion in various grades of vegetable and waste oils used for bio-fuel production," *Corrosion Science*, vol. 206, 2022. doi: <https://doi.org/10.1016/j.corsci.2022.110501>
- [24] E. Hu, Y. Xu, X. Hu, L. Pan, and S. Jiang, "Corrosion behaviors of metals in biodiesel from rapeseed oil and methanol," *Renewable Energy*, vol. 37, no. 1, pp. 371-378, 2012. doi: <https://doi.org/10.1016/j.renene.2011.07.010>
- [25] E. Balci, "Investigation of bio-corrosion behavior, structural and thermal properties of Ni₂₀Ti₅₀Sn₃₀ high-temperature shape memory alloy," *Journal of Thermal Analysis and Calorimetry*, vol. 149, no. 17, pp. 9085-9093, 2024. doi: <https://doi.org/10.1007/s10973-024-13376-1>